Visualisation of Horizontal Settling Slurry Flow Using Electrical Resistance Tomography

Kun Li and Yan Han

April 22, 2019

Visualisation of Horizontal Settling Slurry Flow Using Electrical Resistance Tomography

Kun Li[1] and Yan Han

Abstract

Settling slurry flow is very common and important in many industries, especially in slurry transportation, which need be monitored in practical operation. An investigation on visualisation of horizontal settling slurry flow in pipeline using electrical resistance tomography is reported in this paper. The internal images of fluid structure were displayed to operators by measuring the solids concentration distribution and solids velocity distribution in the pipe cross-section. Experimental investigation with 5% solids loading concentration at various transport velocities were conducted. Results obtained from electrical resistance tomography were compared with the results of photography and other flow measurement methods.

Keywords Flow visualisation, Horizontal settling slurry flow, Electrical resistance tomography, Local solid concentration, Local solid velocity

1 Introduction

The transportation of settling slurry flow is required in a variety of industries, such as mining, nuclear, energy, pharmaceutical, chemical and food industries [1-4]. Especially in some specific applications, hydraulic transport through pipes is the only way to transport solid particles. As the slurry is an essential mixture of solids and liquids, its characteristics depend on many factors, such as size and orientation of pipes, size and concentration of solids, velocity and viscosity of the liquid carrier. Therefore, slurry transportation is a highly complex process [2]. Because appropriate slurry flow parameters can efficiently avoid pipe blockage, equipment failures,

[1] K. Li(✉) Y. Han
Shanxi Key Laboratory of Signal Capturing and Processing, North University of China, Taiyuan, China
E-mail: lk_nuc@163.com

and environmental damage, the slurry transportation should be under measurement and monitoring in the transport process. With good understanding of the internal structure of the slurry flow, the optimal design, accurate analysis, and safe operation of slurry transportation systems can be more easily achieved.

Due to the complex nature of slurry flow and the effect of gravity, it is very difficult to measure and visualise the settling slurry flow. In the past, venturi meter [5] based on differential pressure technique was widely used for measuring fluid flow rate. And conductivity probes [6] were installed inside pipes to measure the solids volumetric concentration, which disturbs the internal structure of slurry flow (i.e. intrusive method), and the abrasive nature of slurry make the probe sensor prone to damage. With significant efforts of worldwide researchers, several non-intrusive methods [7-10] appeared, such as, optical (laser) methods, nuclear (X-ray or gamma ray) methods, ultrasound and conductance methods. Among the above methods, electrical resistance tomography (ERT) offered a good solution for measuring and visualising settling slurry flow, since optical methods cannot measure muddy fluids, and nuclear method is expensive and radioactive.

Phase volume fraction and phase velocity are two important parameters to describe the internal structure of slurry flow, and flow characteristics also can be extracted from them, for example flow regimes [3]. With the ERT online measurement, the real-time solids concentration and velocity distribution are offered, which allows process operators to "see" inside the pipe and determine flow conditions. The information can be used to understand and manage slurry flow, and they also provide an experimental basis for CFD and other models in complex flows. Therefore, this paper focuses on the visualisation of horizontal settling slurry flow, where local solids volumetric concentration and local solids axial velocity are measured using an ERT system.

2 Horizontal Settling Slurry Flow Regimes

The flow regime describes the solids spatial distribution of settling slurry, which is crucial for design, optimisation and the control of slurry flow processes. In horizontal settling slurry flow, with the influence of gravity and various flow velocities, the separation of phases occurs and four main flow regimes (from high velocity to low velocity) are developed, namely pseudo-homogeneous, heterogeneous, moving bed and stationary bed [2], as shown in Fig. 1.

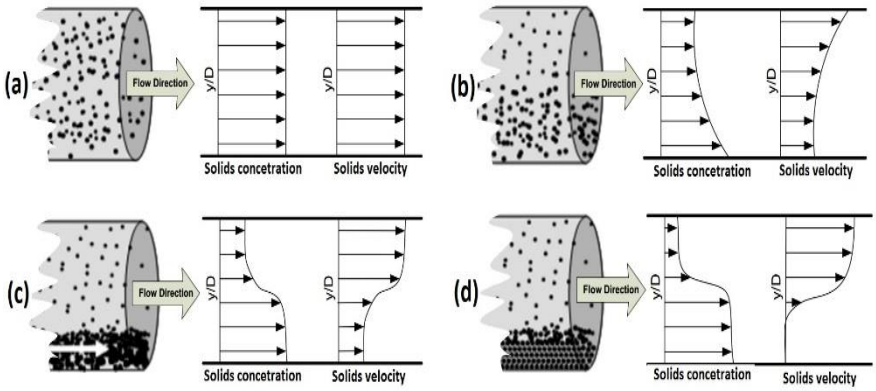

Fig. 1 Schematic presentations of horizontal slurry flow regimes with solids concentration and axis velocity profile. (**a**) Pseudo-homogeneous flow regime. (**b**) Heterogeneous flow regime. (**c**) Moving bed flow regime. (**d**) Stationary bed flow regime.

Homogeneous flow regime usually occurs at high velocities, where fine solid particles are fully suspended in the liquid carrier, as shown in Fig. 1a. As the solid particles are almost evenly distributed and flow with same velocity from the top to the bottom of pipe, it can be approximately regarded as single phase flow, which allows the equivalent fluid model used to represent this type of flow. This flow regime is the mostly commonly used one in industrial applications. As the flow velocity decreases, heterogeneous flow regime occurs, where the solids concentration gradient and axis solid velocity gradient appears in the cross-section of the pipe. As shown in Fig. 1b, the flow regime is referred to as an intermediate flow regime, or might be in the process of forming a flowing bed, where some finer particles are suspended at the top part of pipe and coarser particles are suspended at the bottom part of pipe. This flow regime is usually applied in mining and dredging applications, but a critical velocity is required to maintain the flow regime, i.e. minimum velocity of liquid carrier. Moving bed flow regime starts being formed when the flow velocity is below the critical velocity, where larger particles accumulate at the bottom of pipe and form a flowing bed, and the upper part of fluid is still heterogeneous mixture with less solids concentration, as shown in Fig. 1c. The solids concentration at bottom is maximum, and decreases from the bottom to top in the pipe cross-section. The solids velocity at upper part is higher than at bottom part. As the flow velocity decreases further, the liquid carrier cannot move the solids on the bed, which will be stationary and contact with the bottom of pipe, as shown in Fig. 1d. With the accumulation of solid particles, the stationary bed turns thicker, which might lead to blockage. Therefore, it is impossible to maintain stationary bed flow regime for very long time, and the stationary bed flow should be avoided in practice.

3 ERT System and Principle

The principle of ERT [11] is based on the concept of Ohm's law: by injecting a certain signal through electrodes pair into a conductive sensing region, and the injected signal will result in boundary voltages on the remaining electrodes. The boundary voltages contain the information of conductivity distribution within the sensing region. The boundary voltages data were collected and used to image the internal structure of multi-phase flow using an image reconstruction algorithm [12].

A typical ERT system [11] is made of the ERT sensor, data acquisition system, and image reconstruction system, as shown in Fig. 2. Each plane of the ERT sensor is a set of equally spaced electrodes mounted around the pipe wall, which is in contact with the fluid, and will not cause any interference with the flow. The data acquisition system consists of signal sources, multiplexer arrays, voltmeters, signal demodulators, which is critical for ERT system since it determines sensing strategy, data accuracy and highest data collection speed. Commonly, an adjacent strategy [13] is used in most ERT systems for generating a set of measured data (i.e.104 independent differential voltages for a16-eletrode sensor). Using a pre-loaded image reconstruction algorithm, each set of measured data were transferred to each frame of internal conductivity distribution, which represents the phase distribution in the pipe cross-section. The finite element mesh of pipe cross-section is shown in Fig. 3.

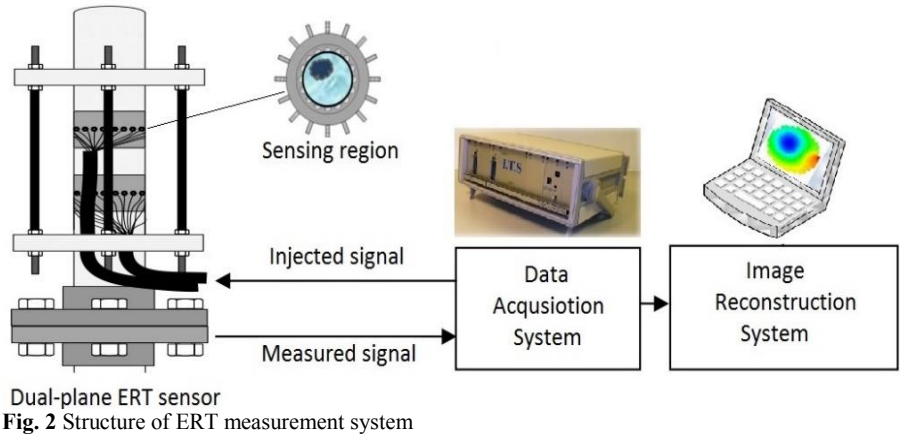

Fig. 2 Structure of ERT measurement system

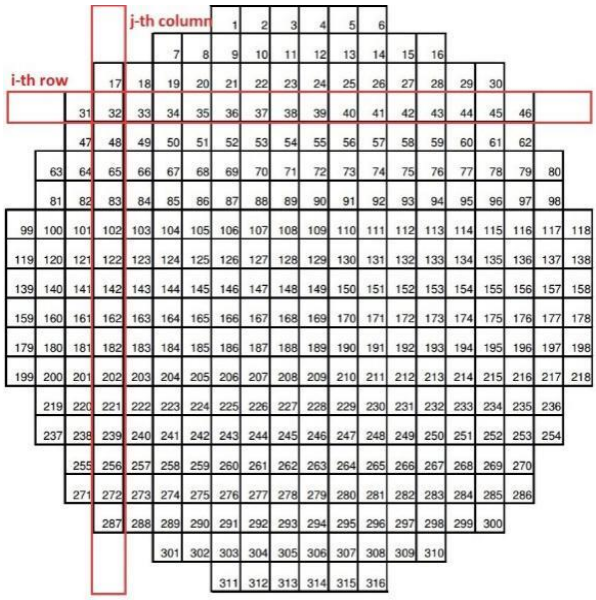

Fig. 3 Finite element mesh (*316 pixels*) of sensing region

Based on simplified Maxwell's relationship for slurry flow [14] (Liquid carrier is water, and solids are silica sand in this paper), the obtained conductivity distribution can be used to derive the solids concentration distribution, as follows.

$$\alpha = \frac{2\sigma_w - 2\sigma_m}{\sigma_w + 2\sigma_m} \tag{1}$$

where, α is the solids concentration in each pixel. σ_w is the conductivity of continuous water phase, and σ_m is the measured mixture conductivity of each pixel.

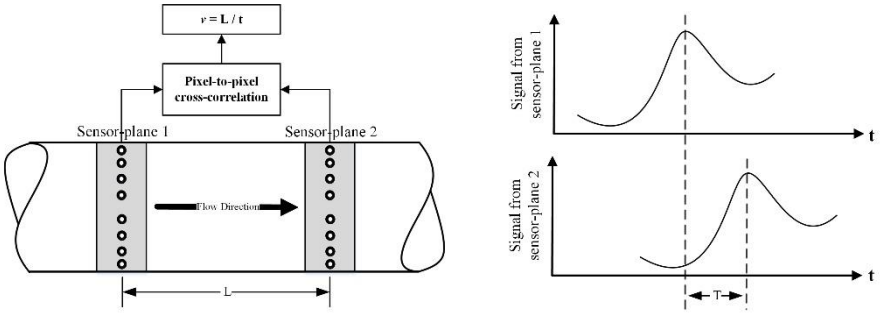

Fig. 4 Principle of Pixel-to-Pixel cross-correlation method

According to the internal conductivity distribution of the dual-plane, the pixel-to-pixel cross-correlation technique [15] is used to measure the time difference of

solid particles flowing through two sensor planes, as shown in Fig. 4. With a predefined distance between the two sensor planes, the solids axial velocity can be calculated using Eq. (2).

$$v = \frac{L}{T} \tag{2}$$

As the horizontal settling slurry flow without stirring can be assumed as vertically axially-symmetric flow, the solids concentration and velocity profile (profile represents the distribution at vertical positions of the pipe cross-section) can be extracted with using the average values of each row, i.e. Eq. (3) and (4). The local mean solids concentration and mean solids velocity can be calculated with the average value of 316 pixels, i.e. Eq. (5) and (6).

$$\alpha_i = \frac{1}{n_i}\sum_{j=1}^{n_i} \alpha_{i,j} \tag{3}$$

$$v_i = \frac{1}{n_i}\sum_{j=1}^{n_i} v_{i,j} \tag{4}$$

$$\bar{\alpha} = \frac{1}{n}\sum \alpha_{i,j} \tag{5}$$

$$\bar{v} = \frac{1}{n}\sum v_{i,j} \tag{6}$$

where, α_i and v_i are the average solids concentration and velocity of the i-th row (i=1,2,...,20), respectively. $\bar{\alpha}$ and $\bar{v}$ are the local solids mean concentration and velocity, respectively. $\alpha_{i,j}$ and $v_{i,j}$ are the local solids concentration and velocity in the pixel of the i-th row and j-th column, respectively.

4 Experiment Setup

Experimental investigation of settling slurry flow was conducted on a slurry flow loop facility at the University of Leeds, as shown in Fig. 5. It consists of a high performance dual-plane ERT system (FICA, built by OLIL) [16] for measuring local solids concentration and velocity, an EMF (OPTIFLUX 4300, from KROHNE) to obtain fluid velocity, and a CMF (OPTIMASS 700 T50, from KROHNE) to obtain slurry mass flow rate. The slurry flow run in experiment with 5% loading solids volumetric concentration at different transport velocity (from 1.5m/s to 4.0m/s), where solid phase is silica sand (particle size is between 75-700 in diameter) and liquid carrier is tap water. Meanwhile, a section of transparent pipe was installed on the slurry flow loop to take photography of slurry flow at each transport velocity.

In order to evaluate the measurement and visualisation of slurry flow with using ERT, the photography results, EMF and CMF results were compared ERT results.

The solids concentration from CMF and EMF measurement can be calculated with Eq. (7).

$$\alpha \cdot \rho_s + (1-\alpha) \cdot \rho_w = \frac{Q}{v \cdot A} \tag{7}$$

where, ρ_s and ρ_w are the density of sand and water, respectively. α is the solids concentration. Q and v are slurry mass flow rate and velocity, respectively. A is the cross-sectional area of the pipe.

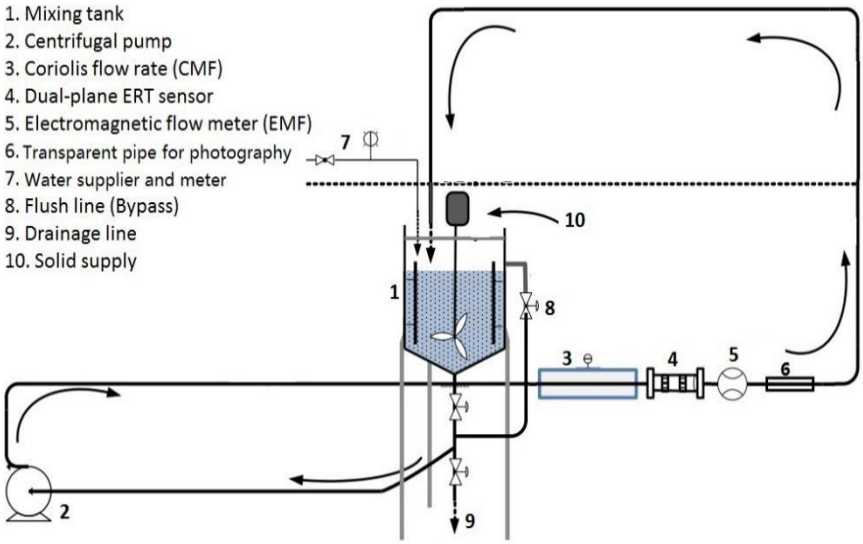

Fig. 5 Experimental facility (*slurry flow loop*) in Leeds University, UK

5 Results and Discussions

Fig. 6 shows the local solids concentration and solids velocity profile with different transport velocities. It can be noticed that the solids distribution and flow conditions depend on the transport velocity. At higher transport velocity, the solid particles are all suspended in slurry mixture, and almost uniformly distributed in the pipe cross-section, as demonstrated at 4.0 m/s in Fig. 7a, and the solids velocities at different positions of the pipe cross-section are almost equal. With the transport velocity decreasing, the solid particles in upper part tend to the lower part, and the velocity of solids particles in lower part slowdown, which tends to form a moving bed. Especially at 1.5 m/s, the solid particles clearly accumulate and move in the lower part, as demonstrated in Fig. 7b, and the solids velocity in moving bed is lower than in the upper part.

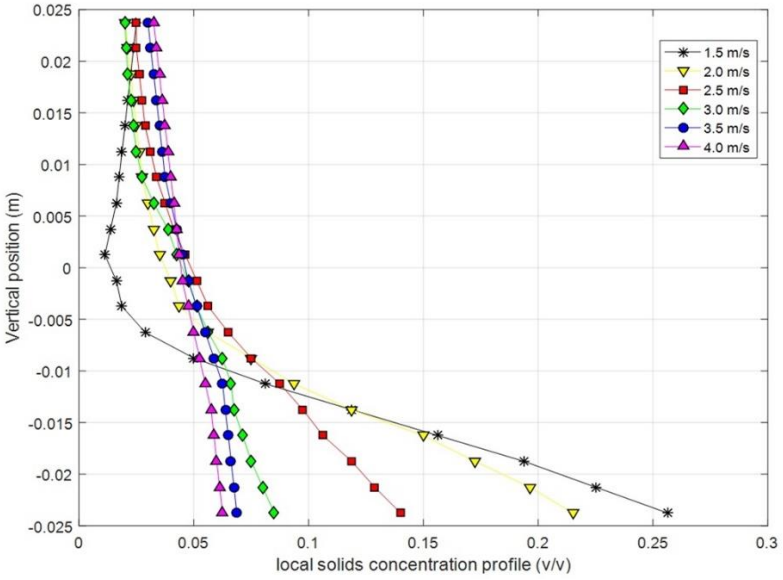

(a)

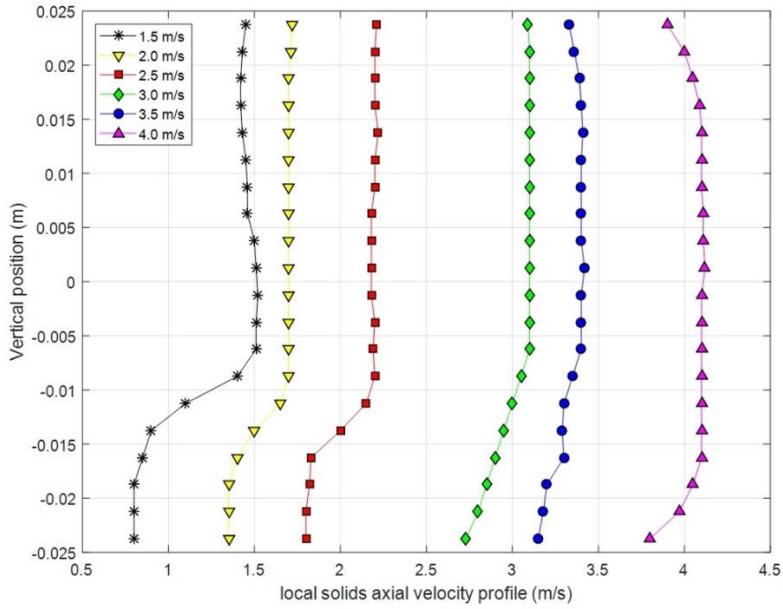

(b)

Fig. 6 Visualisation of slurry flow with 5% sand (*transport velocities (from 1.5 m/s to 4.0 m/s*) (**a**)Local solids concentration profile (**b**) Local solids velocity profile

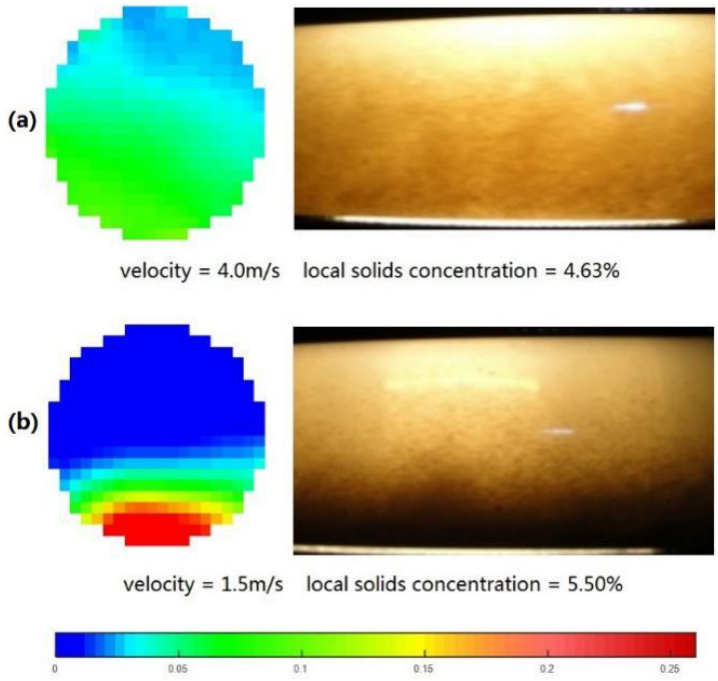

Fig. 7. Local solids concentration distribution in the pipe cross-section and photography of slurry flow. (**a**) Slurry flow at 4.0 m/s transport velocity. (**b**) Slurry flow at 1.5 m/s transport velocity.

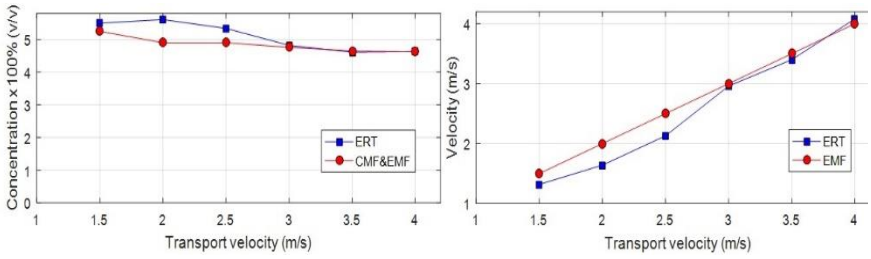

(a) (b)

Fig. 8. Error analysis. (**a**) Comparison of local solids concentration obtained from ERT with that of CMF and EMF, (**b**) Comparison of solids velocity obtained from ERT and transport velocity measured by EMF

Fig. 8a shows that the local mean solids concentration obtained from ERT and from EMF and CMF are similar, which implies that the ERT provides a reasonable method to visualise slurry flow. Fig. 8b shows that the mean solids velocity obtained from ERT are consistent with the transport velocity at high velocity (especially over 3.0 m/s). However, as the increase of solids concentration in pipe bottom leads to a strong particle-particle interaction at low velocity (below 2.5 m/s), the movement

of solid particles is impeded, and the solids velocity is lower than transport velocity, which is highlighted by the ERT.

6 Conclusions

A visualisation method using a high performance ERT system on horizontal settling slurry flow was investigated. It demonstrated that ERT can determine the mean local solids concentration and solids concentration profile at vertical positions of pipe cross-section, which shows the amount and the distribution of solid particles in slurry. With cross-correlation technique, the dual-plane ERT system can determine the mean local solids velocity and solids velocity profile in pipe. The ERT results were compared with actual photography and other flow measurement methods, which verified the dual-plane ERT system colud perform well for visualising slurry flow in pipeline. Meanwhile, the below conclusions were drawn:

- Compared with photography and other flow measurement methods, ERT offers a better solution for monitoring slurry flow, as the solids concentration distribution and velocity distribution were clearly shown in ERT results.
- At slow slurry transparent velocity, the solids velocity in lower part of pipe is slower than in upper part, and the mean local solids velocity is smaller than transparent velocity, which are highlighted in ERT results.

Acknowledgments The authors would like to express their gratitude for the support from the Chinese Scholarship Council (CSC) and the School of Chemical and Process Engineering, who made Mr. Li's study at the University of Leeds possible.

References

1. Stanley S J, Bolton G T (2010) A review of recent electrical resistance tomography (ERT) applications for wet particulate processing. Particle & Particle Systems Characterization, 25(3), 207-215
2. Abulnaga B (2002) Slurry Systems Handbook. McGraw-Hill. ISBN 0-07-137508-2
3. Robert C, Ramsdell (2013) An overview of flow regimes describing slurry transport. Proceedings of the Art of Dredging. Brussels, Belgium
4. Kaminoyama M (2014) Review of visualization of flow and dispersion states of slurry system fluids in stirred vessels. Journal of Chemical Engineering of Japan, 47(2), 109-114
5. Shook C A, Masliyah J H (2010) Flow of a slurry through a venturi meter. Canadian Journal of Chemical Engineering, 52(2), 228-233
6. Nasr-El-Din H, Shook C A, Colwell J (1987) A conductivity probe for measuring local concentrations in slurry systems. International Journal of Multiphase Flow, 13(3), 365-378
7. Schmidt M, Münstedt H, Svec M, Roosen A, Betz T, Koppe F (2010) Local flow behavior of ceramic slurries in tape casting, as investigated by laser-doppler velocimetry. Journal of the American Ceramic Society, 85(2), 314-320
8. Shimada T, Habu H, Seike Y, Ooya S, Miyachi H, Ishikawa M (2007) X-ray visualization measurement of slurry flow in solid propellant casting. Flow Measurement & Instrumentation, 18(5), 235-240

9. Krupička J, Matoušek V (2014) Gamma-ray-based measurement of concentration distribution in pipe flow of settling slurry: vertical profiles and tomographic maps. Journal of Hydrology & Hydromechanics, 62(2), 126-132
10. Stener J F, Carlson J E, Sand A, Pålsson B I (2016) Monitoring mineral slurry flow using pulse-echo ultrasound. Flow Measurement & Instrumentation, 50, 135-146
11. Wang M (2015) Industrial Tomography: Systems and Applications. Woodhead Publishing, Limited. ISBN 978-1-78242-118-4
12. Li Y, Cao S, Man Z, Chi H (2011) Image reconstruction algorithm for electrical capacitance tomography. Information Technology Journal, 10(8), 269-291
13. Wang M, Wang Q, Bishal, K (2016) Arts of electrical impedance tomographic sensing. Philosophical Transactions, 374(2070), 20150329
14. Wang M, Jones T F, Williams R A (2003) Visualization of asymmetric solids distribution in horizontal swirling flows using electrical resistance tomography. Chemical Engineering Research & Design, 81(8), 854-861
15. MOSAIC Scientific Ltd (2009) AIMFlow Standard Version 1.0 User Manual MOSAIC Scientific Ltd
16. Wang M, Ma Y, Holliday N, Dai Y, Williams R A, Lucas G (2005) A high-performance EIT system. IEEE Sensors Journal, 5(2), 289-299